Nanoscale

ROYAL SOCIETY OF CHEMISTRY

COMMUNICATION

View Article Online
View Journal | View Issue

Cite this: *Nanoscale*, 2023, **15**, 8597

Received 8th March 2023,
Accepted 14th April 2023

DOI: 10.1039/d3nr01091k

rsc.li/nanoscale

Strong fluorescence-detected two-photon circular dichroism of chiral gold nanoclusters†

Anna Pniakowska, Marek Samoć and Joanna Olesiak-Bańska *

Progress in syntheses and understanding of the intriguing properties of chiral noble metal nanoclusters sparks interest to extend investigations of their chiroptical response to the nonlinear optics regime. We present a quantitative determination of two-photon circular dichroism of chiral gold nanoclusters with ATT and L- or D-Arg ligands (ATT = 6-aza-2-thiotymine and Arg = arginine). Introduction of arginine ligands enables the formation of two enantiomers of the nanoclusters, with strong chiroptical effects in both linear and nonlinear regime. We present two-photon absorption and luminescent properties measured in a wide range of wavelengths, with the two-photon absorption cross section reaching 1743 GM and two-photon brightness ~1102 GM at 825 nm. We report strong, 245-fold enhancement of the two-photon circular dichroism of nanoclusters with respect to the one-photon absorption counterpart – the dissymmetry factor. The presence of multiple advantages of nanoclusters: high fluorescence quantum yield, strong nonlinear optical properties and well-controlled chirality is a powerful combination for applications of such clusters in multiphoton microscopy.

Chirality is a common natural attribute, which refers to the objects with non-superimposable mirror image[1] and, since it is exhibited by biomolecules such as amino acids, proteins, sugars and nucleic acids, there is much interest in both exploiting the properties arising from the chirality in bio-applications and in mimicking the natural chirality in new functional nanomaterials and nanostructures. Recent raise of the interest in chirality at nanoscale is motivated by the needs of chirality-based applications, *e.g.* enantioselective separation,[2] catalysis,[3] bioimaging,[4] sensing,[5] and theranostics.[6]

Inspired by this significant interest in fundamental studies and emerging applications of chiral nanomaterials, we have decided to explore in detail the chiroptical properties of gold nanoclusters (AuNCs) taking advantage of their luminescent properties. Nanoclusters are defined as ultra-small, 1–2 nm sized nanoobjects. They consist of a few to a few hundred noble metal atoms, stabilized by a precise number of ligands. Due to discrete character of their electronic energy levels and the absence of localized surface plasmon excitations, the gold nanoclusters differ from the bigger metal nanoparticles and demonstrate unusual optical properties in both linear and nonlinear regime.[7] Features like high luminescence yield and several orders of magnitude stronger two-photon absorption cross sections of nanoclusters[8] against other, well-known nonlinear absorbers[9] initiated the development of strategies for fabrication of nanoclusters with the desired enhanced optical properties.

Chiroptical activity of AuNCs was observed for the first time by Schaaff and Whetten.[10] Up to date a significant progress has been made concerning introduction and investigation of chiroptical properties of such clusters.[11,12] A common strategy for inducing chirality of nanoclusters is protection of their metal core with optically active ligands, *e.g.* L-glutathione (L-GSH),[10] L-captopril,[13] D-/L-penicillamine (Pen),[14] 2,2′-bis (diphenylphosphino)-1,1′-binaphthyl (BINAP)[15] and bidentate 1,1′-binaphthyl-2,2′-dithiol (BINAS).[16] However, the chiral properties of NCs (the circular dichroism) are predominantly established in the UV/Vis range, while various applications, *e.g. in vivo* bioimaging, biosensing, and theranostics favour near-infrared (NIR) excitation. Therefore, one is tempted to consider the multiphoton excitation, which provides low phototoxicity, deeper penetration into samples and higher axial resolution: the features that are strongly beneficial for those applications. AuNCs present a combination of characteristics favourable for multiphoton microscopy: large two-photon absorption cross-sections[7,8] and bright luminescence, together with ultra-small sizes and good biocompability.[17,18] Owing to the listed features, gold nanoclusters have already proved to be robust biosensors and biomarkers for multiphoton applications.[19,20]

Institute of Advanced Materials, Wroclaw University of Science and Technology, Wybrzeże Wyspiańskiego 27, 50-370 Wroclaw, Poland.
E-mail: joanna.olesiak-banska@pwr.edu.pl

† Electronic supplementary information (ESI) available. See DOI: https://doi.org/10.1039/d3nr01091k

Arg/ATT-AuNCs, *i.e.* clusters stabilized with two ligands: 6-aza-2-thiotymine (ATT) and arginine (Arg) are water soluble nanoclusters with particularly high photoluminescent quantum yield, which has recently been successfully applied in imaging[21,22] and detection of arginase activity.[23] Large nonlinear optical (NLO) potential of proposed nanoclusters was recently found in multiphoton *in vivo* bioimaging of living cells with Arg/ATT-AuNCs[24] and silver doped ATT-AuNCs.[25] Despite impressive multiphoton investigations, chiroptical properties of these clusters have not been investigated, neither in linear nor nonlinear regime. In fact, NLO chirality of nanoclusters have been yet poorly investigated, although one-photon chirality of nanoclusters already gained a lot of interests.

Our previous studies on two-photon circular dichroism of $Au_{25}(Capt)_{18}$ NCs was first and currently the only work on NLO chirality of nanoclusters. It have shown a significantly higher anisotropy factor in the regime of two-photon *vs.* one-photon absorption, which inspired us to further investigation of two-photon circular dichroism in gold nanoclusters.[13] Two-photon circular dichroism (TP-CD) denoted here as θ_{TPCD}, can be defined as the difference in the two-photon absorption cross-section (σ_2) for left-handed and right-handed circularly polarized incident light, normalized with the average two-photon absorption cross-section:

$$\theta_{TPCD} = 2\frac{\sigma_{2,L} - \sigma_{2,R}}{\sigma_{2,L} + \sigma_{2,R}}. \quad (1)$$

More generally, the nonlinear circular dichroism can be defined to include other types of nonlinear absorption, like multiphoton absorption or absorption saturation. The nonlinear circular dichroism has been discussed in theoretical works,[26,27] but the experimental studies of the phenomenon have been scarce and concerned a limited group of materials, *e.g.* lanthanides,[28] naphthols,[29] helicene derivatives,[30] and ruthenium salts,[31] which not include nanoclusters.

In this work we propose for the first time the use of fluorescence-detected circular dichroism (FDCD) for examination of nonlinear chiroptical properties of nanoclusters. In general, one-photon FDCD can serve as a complementary technique to absorption based measurements of the circular dichroism (Scheme 1). Fluorescence intensity is directly proportional to the rate of absorption of photons, where the proportionality constant involves the quantum yield of emission. When the quantum yield is assumed to be independent on the polarization of light, the circular dichroism strength can be derived from a difference of fluorescence intensity for left and right-handed circularly polarized light illumination.[32] Introducing higher order processes of circular excitation presumably affects the magnitude of processes observed in linear regime.

While the technique of FDCD is applicable solely to optically active fluorescent samples, it is attractive since it assures better sensitivity and selectivity than absorption-based CD measurements.[33,34] Many sources claim that fluorescence-based techniques provide superior sensitivity since the measurements can be performed at lower concentrations.[33,35]

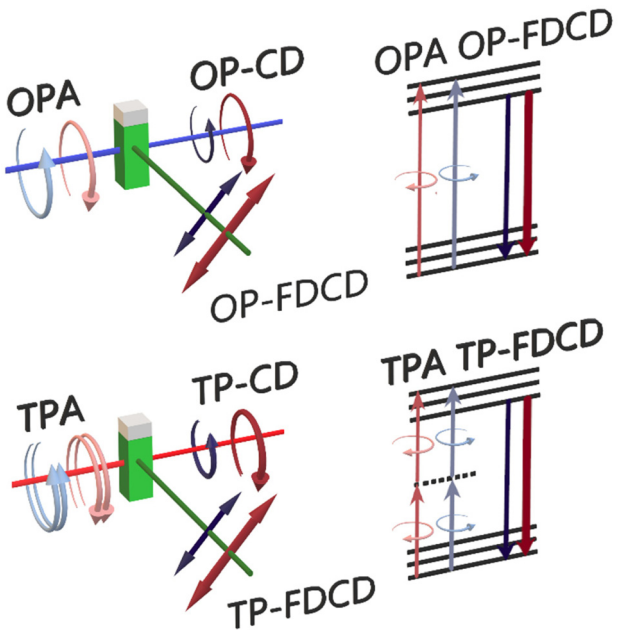

Scheme 1 Scheme of one-photon (OP) and two-photon (TP) circular dichroism (CD) and fluorescence detected circular dichroism (FDCD) effects. Left and right circularly polarized OP and TP excitation can be formed by periodically modulating polarization of the beam (*e.g.* using a photoelastic modulator, PEM) or created separately (*e.g.* using a quarter-wave plate or a Babinet–Soleil compensator). The linear polarization of the photoluminescence indicated by the arrows in the picture does not implicate that it has this polarization as emitted, but that it is detected after passing through a polarizer positioned at a magic angle.

Moreover, FDCD eliminates scattering artifacts generated in absorption detected CD and provides stronger CD response as soon as the samples exhibit quantum yield (QY) > 0.1–0.2.[32,34] Despite the appealing potential of this technique, application of FDCD is limited by complex conditions of measurements in order to obtain explicit results. One must be aware that major artifacts may be generated in FDCD by the presence of residual linear polarization in incident circularly polarized light.[36,37] Yet, FDCD already appeared as a useful tool for determination of conformational and structural changes of the samples, unmeasurable using common CD spectroscopy.[34,37]

Here, we introduce the fluorescence-based technique of chirality measurements to nonlinear optical spectroscopy. We established a protocol of TP-FDCD measurements on a modified two-photon excited luminescence (TPEL) optical set-up. We present an expanded characterization of TP-FDCD of specifically chosen – strongly luminescent and chiral gold nanoclusters of L- and D-Arg/ATT-AuNCs, which optical properties have not been yet considered in two enantiomeric forms of ligands, neither in linear and nonlinear regime. Multiphoton studies have been provided in broad NIR range instead of common characterization at single excitation wavelength. We also compare TP-FDCD to one-photon CD characterization of gold nanoclusters. Our study shows more than 245-times enhanced two-photon luminescence-detected circu-

lar dichroism (θ_{TPCD}) compared to the one-photon dissymmetry factor (g_{abs}).

Results and discussion

Chiral gold nanoclusters Arg/ATT-AuNCs, stabilized with 6-aza-2-thiotymine and arginine, were synthesized according to the previously reported procedure[38] with minor modifications (see ESI†). We established their average diameter to be equal to 1.89 ± 0.28 nm and 1.94 ± 0.29 nm for ATT-AuNCs and L-Arg/ATT-AuNCs, respectively, using Transmission Electron Microscopy (TEM) (Fig. S1†). Thus, no significant change in the diameters of nanoclusters before and after addition of Arg was observed.

One-photon absorption spectrum of ATT-protected nanoclusters presents two absorption bands, at 415 nm and 480 nm. Addition of Arg causes sharpening and shifting of the former band to 405 nm and splitting of the latter band into well resolved peaks around 466 nm and 505 nm for L/D-Arg/ATT-AuNCs (Fig. 1), which is in good agreement with recent reports.[38,39] Fig. S2† present differences in band-gap energies. Excitation spectra shown in Fig. S3† resemble the same well separated transition bands.

Addition of Arg does not shift the emission maximum (λ_{max} = 528 nm), however, it strongly influences the photoluminescence (PL) intensity: 45- and 43-fold enhancement of PL for L-Arg/ATT-AuNCs and D-Arg/ATT-AuNCs, respectively, is observed, with respect to ATT-Au NCs. The strong green fluorescence observed under UV light irradiation is shown in the inset of Fig. 1. Dramatically enhanced PL properties of NCs stabilized with Arg can be explained by rigidification of their structure *via* host–guest assemblies, formed by hydrogen bonds between ATT ligand and guanidine group of Arg.[38] Supramolecular interaction of Arg and ATT-AuNCs hinders the intramolecular vibration and rotation of ATT and reduces the non-radiative relaxation of excited states, resulting in enhanced photoluminescence. Strong improvement of luminescent properties is also observed in PL lifetime characterization: 7 ns PL decay time of AuATT NCs is elongated to 42 ns after functionalization with Arginine. The PL decay curves of the NCs are well fitted with biexponential model (eqn (7) and (8), ESI†) as shown in Fig. S4 and Table S1.† We also examined the QY in a direct QY measurement using an integrating sphere. The values determined for L-Arg/ATT-AuNCs and D-Arg/ATT-AuNCs were Φ = 63.2 ± 2.0% and Φ = 58.4 ± 2.0%, respectively. The QY of AuATT NCs was below the integrating sphere sensitivity, therefore the QY of uncoated AuNCs was determined using a comparative method with respect to fluorescein, obtaining Φ = 1.4 ± 0.3%. Our values of QY and PL lifetime of both enantiomers correspond well with the values determined for L-Arg/ATT-AuNCs reported previously.[39] Analysis of radiative and nonradiative rate constants (k_r and k_{nr}) from QY and PL lifetime confirm enhanced radiative or reduced non-radiative processes after functionalization with Arg (Table S1†).

Fig. S5† shows CD spectra of Arg/ATT-AuNCs, which present distinct mirror images for L- and D-form of Arg/ATT-AuNCs with strongest CD peaks around 350 nm, 415 nm and 470 nm, which differ from the CD response of pure L-Arg and D-Arg ligands themselves. ATT-AuNCs are nonchiral nanoclusters therefore they do not generate any CD signal. The one-photon anisotropy factor g_{abs} (Fig. 2a) was determined according to eqn (1) in Experimental section, ESI.† The chiroptical properties of any enantiomeric forms of Arg/ATT-AuNCs have not been reported in the literature, but the magnitude of g_{abs} is comparable with the values common for other gold nanoclusters stabilized with chiral ligands.[40,41] Zhong *et al.* proposed most probable structure of ATT-AuNCs and Arg/ATT-AuNCs,[42] which shows unique structure organisation, that may suggest the origin of chirality being in chiral arrangement of ligands.

Fluorescence detected circular dichroism was measured on a custom-built TP-FDCD system presented in Fig. S6.† We optimized the procedure of TP-FDCD measurements in order to compensate for any depolarization and artefacts, as described in detail in the ESI.† Briefly, left- and right-circularly polarized laser beam was formed using a Babinet–Soleil compensator to eliminate any linear polarization contribution. To ensure the best quality of polarization, a Glan-Thompson polarizer was introduced at the entrance of the optical path. Following the principles given by Tinoco[35] and Bain,[36] during one-photon and two-photon FDCD measurements the luminescence was collected at so-called *magic angle* of 54.7°, which is positioned between the propagation vector of the laser and the polarizer axis,[32,36] as shown in Fig. S6.† It is assumed that the fluorescence of axially symmetric systems provides equivalent response in every direction of luminescence polarization.

Examples of two-photon excited luminescence spectra of the chiral nanoclusters and achiral fluorescein are collected in Fig. S7† to indicate the impact of left- and right-circularly polarized excitation. Owing to the opposite chirality of two

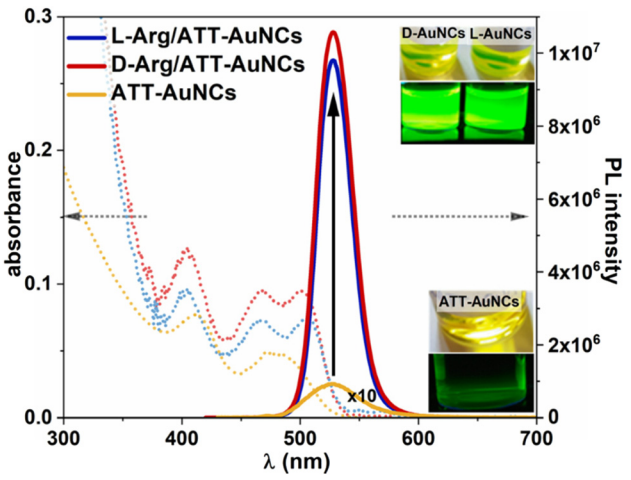

Fig. 1 Absorption and emission spectra of ATT-AuNCs and two enantiomeric forms of Arg/ATT-AuNCs. Solid black arrow indicates PL enhancement of nanoclusters after addition of Arg to ATT-AuNCs. Photographs in the inset present eye-visible green luminescence.

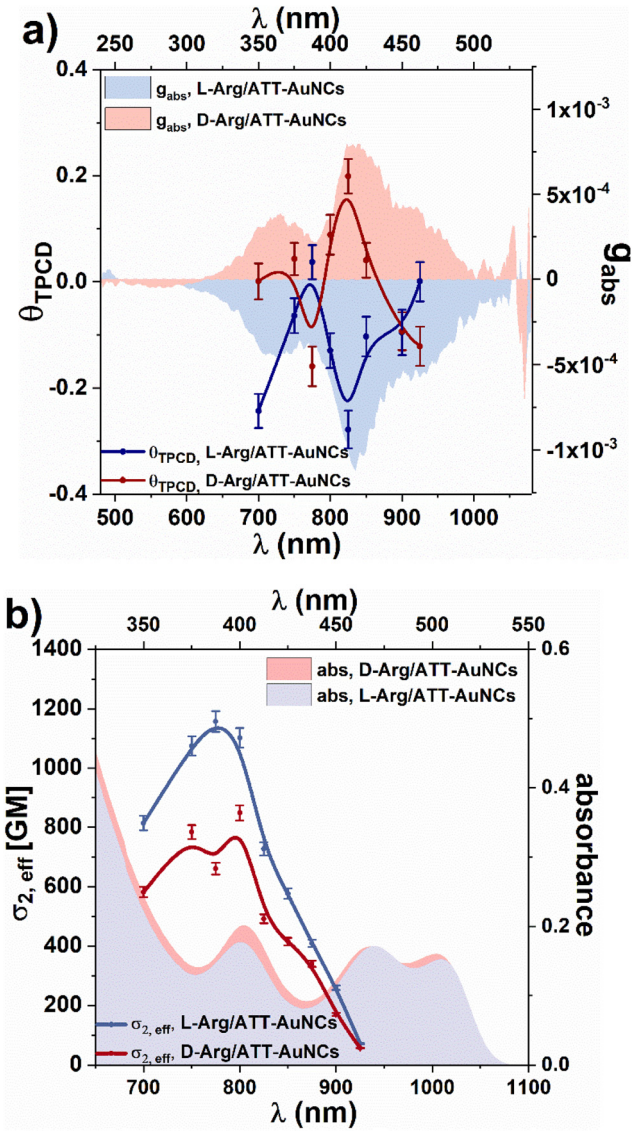

Fig. 2 (a) Two-photon circular dichroism (blue and red dots and lines, left and bottom axes) correlated with one-photon dissymmetry factor (blue and red areas, right and upper axes). (b) Two-photon brightness spectra of L-Arg/ATT-AuNCs and D-Arg/ATT-AuNCs (blue and red dots and lines, left and bottom axes) correlated with absorption of those nanoclusters(blue and red areas, right and upper axes).

enantiomeric nanoclusters, different PL intensities are detected depending on the direction of circularly polarized excitation (Fig. S7a and b†). We used fluorescein solution as a reference sample, which, in a properly calibrated FDCD set-up, provides identical two-photon luminescence intensity for left- and right-handed circular polarization (Fig. S7c†). To validate two-photon character of luminescence we performed laser power-dependent photoluminescence intensity measurements, which results in quadratic dependence of log–log plots (Fig. S8†).

To evaluate the potential of nanoclusters in two-photon chiroptical sensing and imaging *via* luminescence we determined the left- and right-handed two-photon brightness ($\sigma_{2,\mathrm{eff}}$), as the product of two-photon absorption cross-section (σ_2) and PL quantum yield, according to eqn (2):

$$\sigma_{2,\mathrm{eff,s}} = \sigma_{2,\mathrm{s}}\varphi_{\mathrm{s}} = \frac{F_{2,s(\lambda_{\mathrm{exc}})}C_{\mathrm{r}}\varphi_{\mathrm{r}}}{F_{2,\mathrm{r}(\lambda_{\mathrm{exc}})}C_{\mathrm{s}}}\sigma_{2,\mathrm{r}}, \quad (2)$$

where φ is the quantum yield, C is the concentration and F is the integrated fluorescence at a particular excitation wavelength for s – sample and r – reference solution. TPA cross-sections are usually quoted in the units of Göppert-Mayer, where 1 GM refers to 10^{-50} cm^4 per s per photon. We determined the two-photon absorption properties in a wide range of 700–930 nm excitation wavelengths. Both enantiomeric forms of nanoclusters present strong two-photon absorption around 750–800 nm that corresponds to respective (one-photon) absorption bands plotted at doubled wavelength (Fig. S9†). The highest values are $\sigma_{2,\mathrm{s}}$ = 1743 GM and 1453 GM for L- and D-Arg/ATT-AuNCs, respectively, they compare favorably with σ_2 reported for other gold nanoclusters examined with the same method of TPEL.[8] Due to strong QY of the fluorescent nanoclusters described here, also their $\sigma_{2,\mathrm{eff}}$ values are very respectable: 1102 GM and 848 GM (Fig. 2b) for L- and D-Arg/ATT-AuNCs samples, respectively, which are several times higher than $\sigma_{2,\mathrm{eff}}$ of other nanoclusters reported in the literature.[43,44] Furthermore, the reported $\sigma_{2,\mathrm{eff}}$ are significantly larger than those for commonly used fluorophores, *e.g.* dyes[45] and fluorescent proteins,[46] suggesting that Arg/ATT-AuNCs are outstanding candidates for multiphoton imaging applications.

Having the left- and right-handed circularly polarized two-photon absorption cross-sections, we could calculate the two-photon circular dichroism θ_{TPCD} according to eqn (1) and contrast it with the one-photon anisotropy factor g_{abs} (Fig. 2a). θ_{TPCD} follows the mirror-image of respective negative and positive bands of g_{abs} L/D-Arg/ATT-AuNCs. It is expected for non-centrosymmetric systems of chiral nanoclusters since OPA and TPA involve the same excited states. The strongest θ_{TPCD} = −0.27 is obtained at 825 nm. It presents ~245-times increased chiroptical response in comparison to the one-photon anisotropy factor at a corresponding wavelength (Table 1). To the best of our knowledge θ_{TPCD} of nanoclusters was studied only once previously, by the *Z*-scan technique. For Au_{25} gold nanoclusters, two orders of magnitude enhancement of the two-photon anisotropy factor was found, as compared to one-photon chiral response.[13] It corresponds well with our findings of θ_{TPCD}, determined with the TP-FDCD technique. The deeper discussion on the nonlinear chiroptical properties would require extensive theoretical study, going beyond the usual point dipoles approximation. Already the first theoretical descriptions of two-photon CD by Power[26] and Bain[36] involved multipolar and magnetic transitions, and further investigations were performed by Rizzo.[47] However, as there are no theoretical and computational studies of circular dichroism of Arg/ATT-AuNCs nanoclusters and no two-photon circular dichroism simulations of any of atomically-precise nanoclusters, a question whether universal theories provide satis-

Table 1 One-photon and two-photon optical and chiroptical characterization of L/D-Arg/ATT-AuNCs

	One-photon		Two-photon		
Sample	integrating sphere QY [%]	g_{abs} (415 nm)	σ_2 [GM] (800 nm)	$\sigma_{2,eff}$ [GM] (800 nm)	θ_{TPCD} [GM] (825 nm)
L-Arg/ATT-AuNCs	63.2 ± 2.0%	-1.1×10^{-3}	1743 ± 52	1102 ± 33	−0.27 ± 0.04
D-Arg/ATT-AuNCs	58.4 ± 2.0%	7.8×10^{-4}	1453 ± 44	848 ± 25	0.19 ± 0.03

factory explanation for nonlinear chiroptic effects in complex systems of chiral nanoclusters cannot be currently answered.

One-photon FDCD of various types of materials proved to follow the CD response with the same quantitative features.[35,48] Determination if two-photon CD enhancement presents a more general trend among nanoclusters and other materials will require in-depth analysis of the chirality of ground and excited electronic energy levels in one-photon and two-photon absorption. As two-photon FDCD is yet poorly examined in the literature, comparison between experimental CD and FDCD studies is lacking, especially for nanomaterials. Thus, our contribution gives a valuable input to the description of chiroptical properties of nanoclusters and we hope it will stimulate further research in this area.

Conclusions

In this work we presented the quantitative description of two-photon circular dichroism of gold nanoclusters established *via* luminescence in a wide range of wavelengths. We evaluated linear and nonlinear optical properties of chiral L-Arg/ATT-AuNCs and D-Arg/ATT-AuNCs. Large two-photon absorption cross-sections (~1743 GM) and two-photon brightness (~1102 GM) confirm excellent NLO properties of these AuNCs. Subsequently, we determined TP-FDCD spectra of these clusters, obtaining maximum values of θ_{TPCD} = −0.27 and 0.19 for L-Arg/ATT-AuNCs and D-Arg/ATT-AuNCs, respectively. Our two-photon FDCD findings revealed over two orders of magnitude enhanced circular dichroism *vs.* one-photon characteristics of L/D-Arg/ATT-AuNCs. Similarity of this finding to the enhancement factor reported for Au_{25} nanoclusters[13] rises a question about how general such boosting of the chiroptical response in two-photon regime is in nanoscale structures. Comparing results of CD and FDCD, the fluorescent technique is indeed found to present stronger sensitivity than the absorption-based one, offering prospective applications in enantioselective imaging, catalysis, sensing or biomedicine.

Author contributions

The manuscript was written through contributions of all authors. AP: methodology, investigation, writing – original draft, visualization; JOB: conceptualization, writing – review & editing, supervision, funding acquisition. MS: conceptualization, writing – review & editing.

Conflicts of interest

There are no conflicts to declare.

Acknowledgements

The authors acknowledge funding from Narodowe Centrum Nauki under grant Sonata Bis 2019/34/E/ST5/00276.

References

1 L. D. Barron, *Molecular Light Scattering and Optical Activity*, Cambridge University Press, Cambridge, 2 edn, 2004.
2 N. Shukla, M. A. Bartel and A. J. Gellman, *J. Am. Chem. Soc.*, 2010, **132**, 8575–8580.
3 S. Jiang, M. Chekini, Z.-B. Qu, Y. Wang, A. Yeltik, Y. Liu, A. Kotlyar, T. Zhang, B. Li, H. V. Demir and N. A. Kotov, *J. Am. Chem. Soc.*, 2017, **139**, 13701–13712.
4 C. Hao, X. Wu, M. Sun, H. Zhang, A. Yuan, L. Xu, C. Xu and H. Kuang, *J. Am. Chem. Soc.*, 2019, **141**, 19373–19378.
5 M. Matuschek, D. P. Singh, H.-H. Jeong, M. Nesterov, T. Weiss, P. Fischer, F. Neubrech and N. Liu, *Small*, 2018, **14**, 1702990.
6 Z. Peng, L. Yuan, J. XuHong, H. Tian, Y. Zhang, J. Deng and X. Qi, *J. Nanobiotechnol.*, 2021, **19**, 220.
7 J. Olesiak-Banska, M. Waszkielewicz, P. Obstarczyk and M. Samoc, *Chem. Soc. Rev.*, 2019, **48**, 4087–4117.
8 V. Bonačić-Koutecký and R. Antoine, *Nanoscale*, 2019, **11**, 12436–12448.
9 P. A. Shaw, E. Forsyth, F. Haseeb, S. Yang, M. Bradley and M. Klausen, *Front. Chem.*, 2022, **10**, 921354.
10 T. G. Schaaff, G. Knight, M. N. Shafigullin, R. F. Borkman and R. L. Whetten, *J. Phys. Chem. B*, 1998, **102**, 10643–10646.
11 Y. Li, T. Higaki, X. Du and R. Jin, *Adv. Mater.*, 2020, **32**, 1905488.
12 Y. Zhu, J. Guo, X. Qiu, S. Zhao and Z. Tang, *Acc. Mater. Res.*, 2021, **2**, 21–35.
13 J. Olesiak-Banska, M. Waszkielewicz and M. Samoc, *Phys. Chem. Chem. Phys.*, 2018, **20**, 24523–24526.
14 H. Yao, T. Fukui and K. Kimura, *J. Phys. Chem. C*, 2008, **112**, 16281–16285.
15 S. Takano and T. Tsukuda, *J. Phys. Chem. Lett.*, 2016, **7**, 4509–4513.
16 S. Knoppe, A. Dass and T. Bürgi, *Nanoscale*, 2012, **4**, 4211–4216.

17 J. Sobska, M. Waszkielewicz, A. Podleśny-Drabiniok, J. Olesiak-Banska, W. Krężel and K. Matczyszyn, *Nanomaterials*, 2021, **11**, 1066.
18 A. Cantelli, G. Battistelli, G. Guidetti, J. Manzi, M. Di Giosia and M. Montalti, *Dyes Pigm.*, 2016, **135**, 64–79.
19 R. Han, M. Zhao, Z. Wang, H. Liu, S. Zhu, L. Huang, Y. Wang, L. Wang, Y. Hong, Y. Sha and Y. Jiang, *ACS Nano*, 2020, **14**, 9532–9544.
20 L. Polavarapu, M. Manna and Q.-H. Xu, *Nanoscale*, 2011, **3**, 429–434.
21 H. Yang, Y. Wu, H. Ruan, F. Guo, Y. Liang, G. Qin, X. Liu, Z. Zhang, J. Yuan and X. Fang, *Anal. Chem.*, 2022, **94**, 3056–3064.
22 S. Bhunia, K. Gangopadhyay, A. Ghosh, S. K. Seth, R. Das and P. Purkayastha, *ACS Appl. Nano Mater.*, 2021, **4**, 305–312.
23 H.-H. Deng, X.-Q. Shi, H.-P. Peng, Q.-Q. Zhuang, Y. Yang, A.-L. Liu, X.-H. Xia and W. Chen, *ACS Appl. Mater. Interfaces*, 2018, **10**, 5358–5364.
24 Z. Wei, Y. Pan, G. Hou, X. Ran, Z. Chi, Y. He, Y. Kuang, X. Wang, R. Liu and L. Guo, *ACS Appl. Mater. Interfaces*, 2022, **14**, 2452–2463.
25 Y. Peng, X. Huang and F. Wang, *Chem. Commun.*, 2021, **57**, 13012–13015.
26 E. A. Power, *J. Chem. Phys.*, 1975, **63**, 1348–1350.
27 F. Hache, H. Mesnil and M. C. Schanne-Klein, *Phys. Rev. B: Condens. Matter Mater. Phys.*, 1999, **60**, 6405–6411.
28 K. E. Gunde and F. S. Richardson, *Chem. Phys.*, 1995, **194**, 195–206.
29 C. Toro, L. De Boni, N. Lin, F. Santoro, A. Rizzo and F. E. Hernandez, *Chem. – Eur. J.*, 2010, **16**, 3504–3509.
30 Y. Vesga, C. Diaz, J. Crassous and F. E. Hernandez, *J. Phys. Chem. A*, 2018, **122**, 3365–3373.
31 H. Mesnil, M. C. Schanne-Klein, F. Hache, M. Alexandre, G. Lemercier and C. Andraud, *Phys. Rev. A*, 2002, **66**, 013802.
32 I. Tinoco, in *Optical Activity and Chiral Discrimination: Proceedings of the NATO Advanced Study Institute held at the University of Sussex, Falmer, England, September 10–22, 1978*, ed. S. F. Mason, Springer Netherlands, Dordrecht, 1979, pp. 57–85, DOI: 10.1007/978-94-015-7644-4_4.
33 M. Thomas, G. Patonay and I. Warner, *Rev. Sci. Instrum.*, 1986, **57**, 1308–1313.
34 T. Nehira, K. Ishihara, K. Matsuo, S. Izumi, T. Yamazaki and A. Ishida, *Anal. Biochem.*, 2012, **430**, 179–184.
35 D. H. Turner, I. Tinoco and M. Maestre, *J. Am. Chem. Soc.*, 1974, **96**, 4340–4342.
36 A. J. Bain and A. J. McCaffery, *J. Chem. Phys.*, 1985, **83**, 2632–2640.
37 E. W. Lobenstine and D. H. Turner, *J. Am. Chem. Soc.*, 1980, **102**, 7786–7787.
38 H.-H. Deng, X.-Q. Shi, F.-F. Wang, H.-P. Peng, A.-L. Liu, X.-H. Xia and W. Chen, *Chem. Mater.*, 2017, **29**, 1362–1369.
39 L. Yang, B. Zhang, L. Fu, K. Fu and G. Zou, *Angew. Chem., Int. Ed.*, 2019, **58**, 6901–6905.
40 Y. Yanagimoto, Y. Negishi, H. Fujihara and T. Tsukuda, *J. Phys. Chem. B*, 2006, **110**, 11611–11614.
41 S. Si, C. Gautier, J. Boudon, R. Taras, G. Serafino and T. Bürgi, *J. Phys. Chem. C*, 2009, **113**, 12966–12969.
42 Y. Zhong, J. Zhang, T. Li, W. Xu, Q. Yao, M. Lu, X. Bai, Z. Wu, J. Xie and Y. Zhang, *Nat. Commun.*, 2023, **14**, 658.
43 A. Pniakowska, K. Kumaranchira Ramankutty, P. Obstarczyk, M. Perić Bakulić, Ž. Sanader Maršić, V. Bonačić-Koutecký, T. Bürgi and J. Olesiak-Bańska, *Angew. Chem., Int. Ed.*, 2022, **61**, e202209645.
44 C.-L. Liu, M.-L. Ho, Y.-C. Chen, C.-C. Hsieh, Y.-C. Lin, Y.-H. Wang, M.-J. Yang, H.-S. Duan, B.-S. Chen, J.-F. Lee, J.-K. Hsiao and P.-T. Chou, *J. Phys. Chem. C*, 2009, **113**, 21082–21089.
45 M. A. Albota, C. Xu and W. W. Webb, *Appl. Opt.*, 1998, **37**, 7352–7356.
46 M. Drobizhev, N. S. Makarov, S. E. Tillo, T. E. Hughes and A. Rebane, *Nat. Methods*, 2011, **8**, 393–399.
47 D. H. Friese, C. Hättig and A. Rizzo, *Phys. Chem. Chem. Phys.*, 2016, **18**, 13683–13692.
48 A. Ben Moshe, D. Szwarcman and G. Markovich, *ACS Nano*, 2011, **5**, 9034–9043.

